

Supplementary Material

Enhancing the Performance of Triboelectric Generator: A Novel Approach Using Solid-Liquid Interface-Treated Foam and Metal Contacts

Quang Tan Nguyen ¹, Duy Linh Vu ², Chau Duy Le ¹ and Kyoung Kwan Ahn ^{2,*}

¹ Graduate School of Mechanical Engineering, University of Ulsan, 93, Daehak-ro, Nam-gu, Ulsan 44610, Republic of Korea

² School of Mechanical Engineering, University of Ulsan, 93, Daehak-ro, Nam-gu, Ulsan 44610, Republic of Korea

* Correspondence: kkahn@ulsan.ac.kr

Table S1. Peak voltage and current density of various mechanical energy harvesters

| Types | Active materials | Size | Voltage (V) | Current density (A/m ²) | Refs |
|-------------------------|--|----------------------|------------------|-------------------------------------|-----------|
| Piezoelectric Generator | C/PDMS/AuNPs | 3.5 cm × 8.5 cm | 6 V | 2.35.10 ⁻⁴ | [62] |
| | CMC/PDMS/CNT | 3.3 cm × 2.5 cm | 30 | 6.06.10 ⁻⁴ | [63] |
| | Cellulose/SbSI | 1 cm × 1 cm | 0.024 | 2.10 ⁻⁴ | [64] |
| | TOCN/PDMS | 1 cm × 2 cm | 60 | 5.05.10 ⁻² | [61] |
| | MoS ₂ /PVDF | 3 cm × 3 cm | 50 | 3.33.10 ⁻⁵ | [65] |
| | ZnO nanowire array | ~2 mm ² | 10 ⁻³ | 7.5.10 ⁻⁵ | [66] |
| Triboelectric Generator | ZnO nanosheets/Zn: Al layered double hydroxide layer | 6 mm ² | 0.38 | 0.217 | [67] |
| | Treated wood | 4.5 cm × 4.5 cm | 81 | 8.89.10 ⁻⁴ | [68] |
| | PCL/GO | 4 cm × 4 cm | 120 | 2.5.10 ⁻³ | [69] |
| | Ppy-MWCNT | 6.25 cm ² | 196.8 | 5.04.10 ⁻² | [70] |
| | CA/PEI/LTV | 5 cm × 5 cm | 478 | 6.30.10 ⁻² | [34] |
| | PA/nylon-66 | 6.8 cm × 7 cm | 4500 | 8.40.10 ⁻³ | [12] |
| | FEP/Cu/Steel/Acrylic/ABS | 7.5 cm × 7 cm | 149.5 | 4.11.10 ⁻³ | [71] |
| | PTFE/Acrylic | 10 cm ² | 33 | 0.065 | [72] |
| Our generator | Cellulose/Water/Al/Cu | 2 cm × 3.5 cm | ~0.55 | 3.57 | This work |

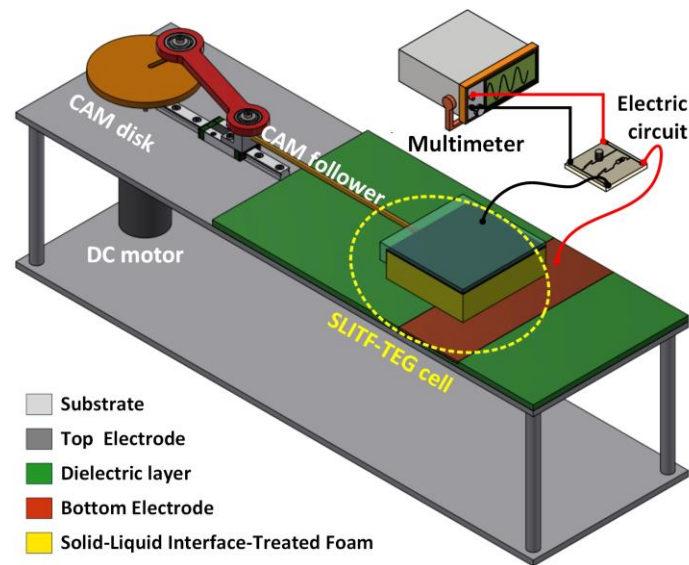


Figure S1. Experimental configuration of the SLITF-TEG

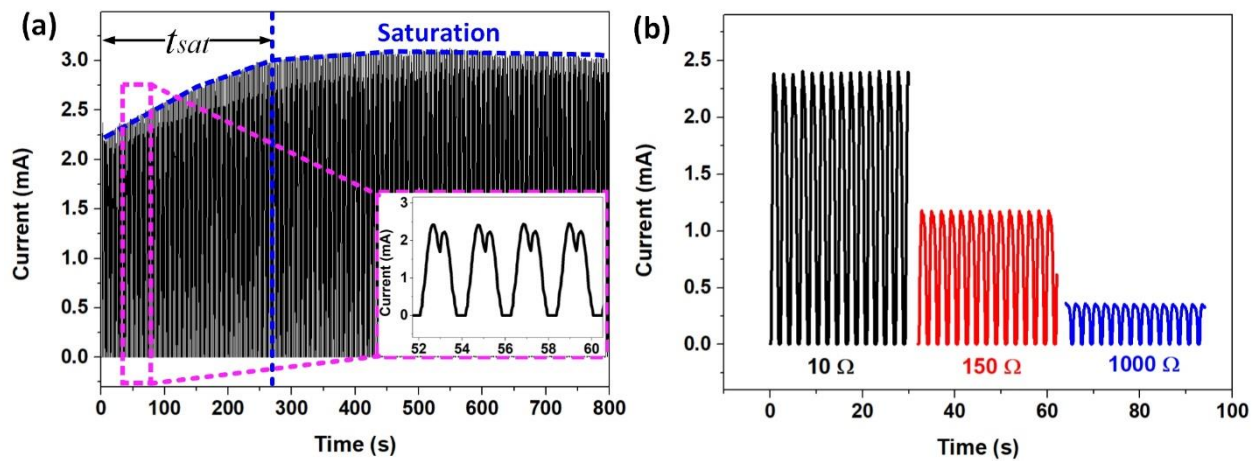


Figure S2. Electrical responses of the SLITF-TEG. The current outputs are measured under (a) the short-circuit condition and (b) various load resistances in the external circuit (10 Ω, 150 Ω, and 1000 Ω).

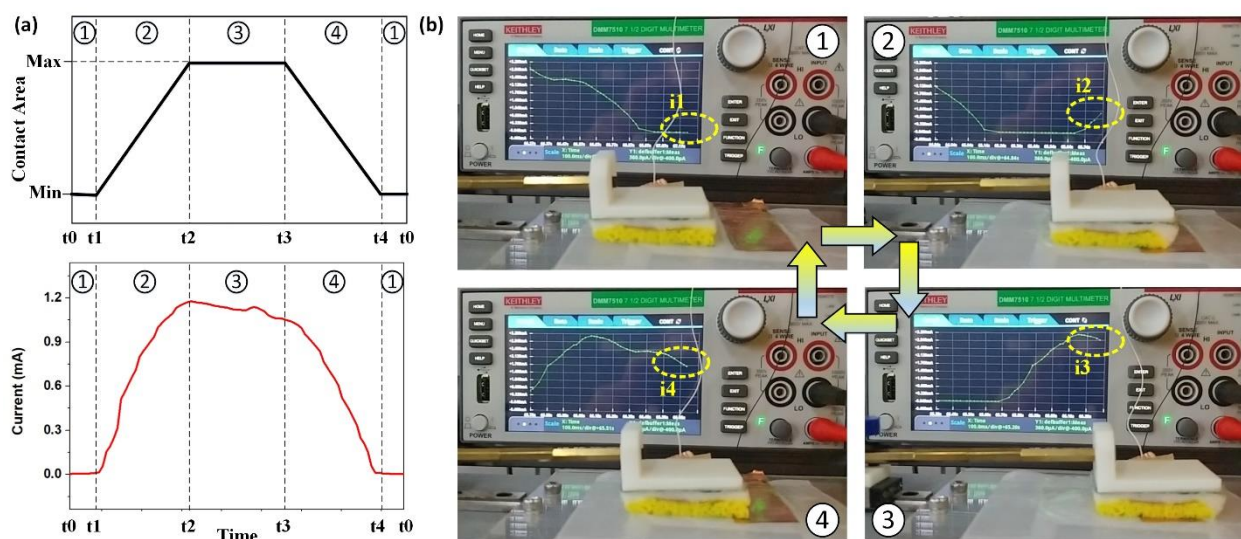


Figure S3. (a) Schematic of the contact area and short-circuit current of the SLITF-TEG. (b) Demonstration of the consistency between the electrical responses and the working mechanism of the SLITF-TEG.

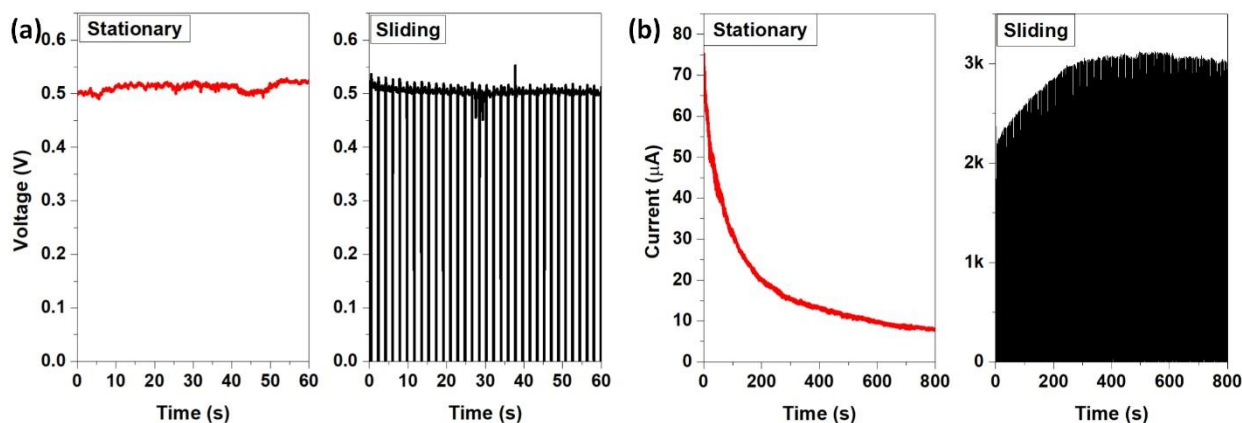


Figure S4. The comparison of (a) open-circuit voltage and (b) short-circuit current of the SLITF-TEG in the stationary and sliding modes.

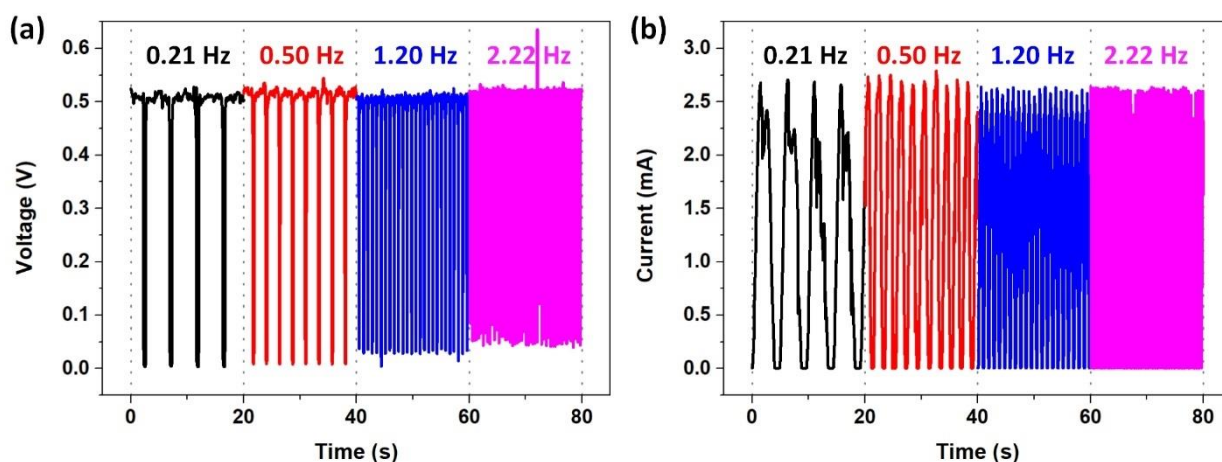


Figure S5. (a) The open-circuit voltage and (b) short-circuit current of the SLITF-TEG under different vibration frequencies.

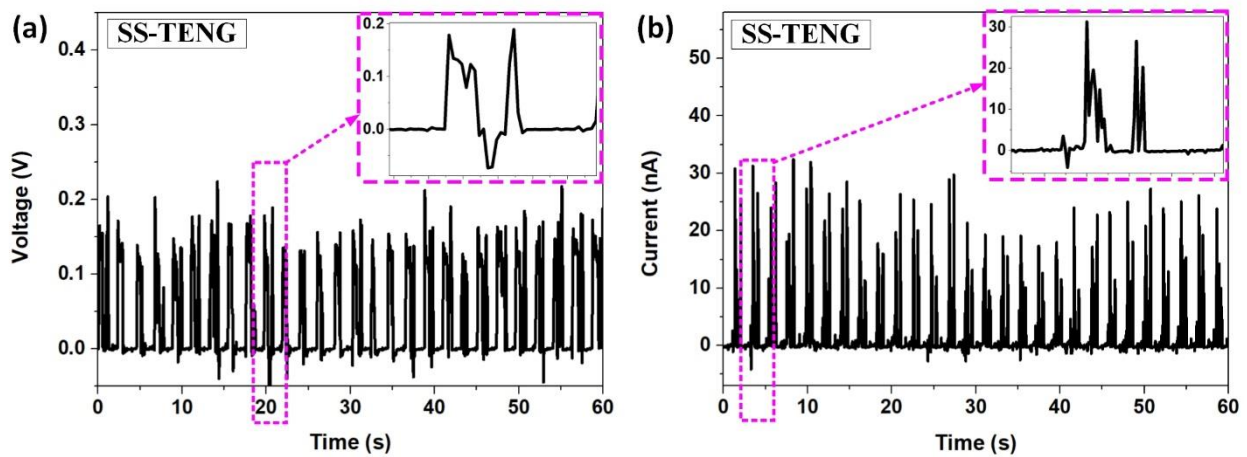


Figure S6. (a) The open-circuit voltage and (b) short-circuit current of the SS-TEG using a dry cellulose foam.

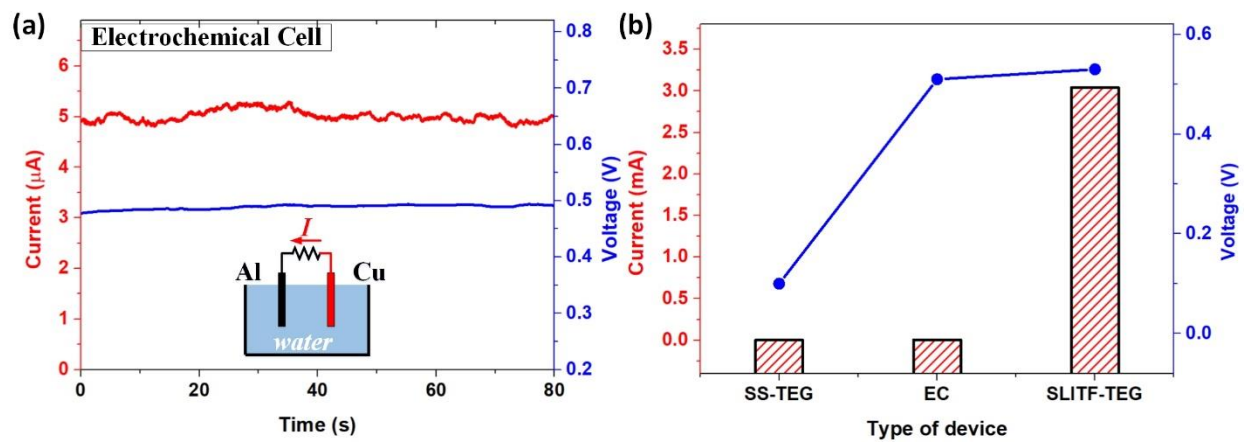


Figure S7. (a) The open-circuit voltage and short-circuit current of an electrochemical cell. (b) The comparison in output performances of SS-TEG, EC, and SLITF-TEG.

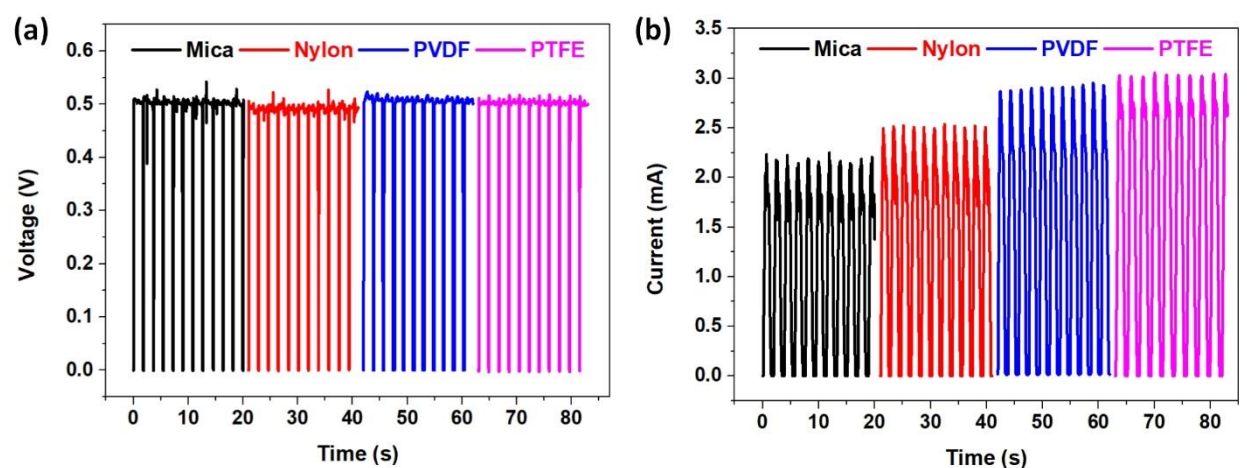


Figure S8. (a) The open-circuit voltage and (b) short-circuit current of the SLITF-TEG using different materials of the dielectric layer.

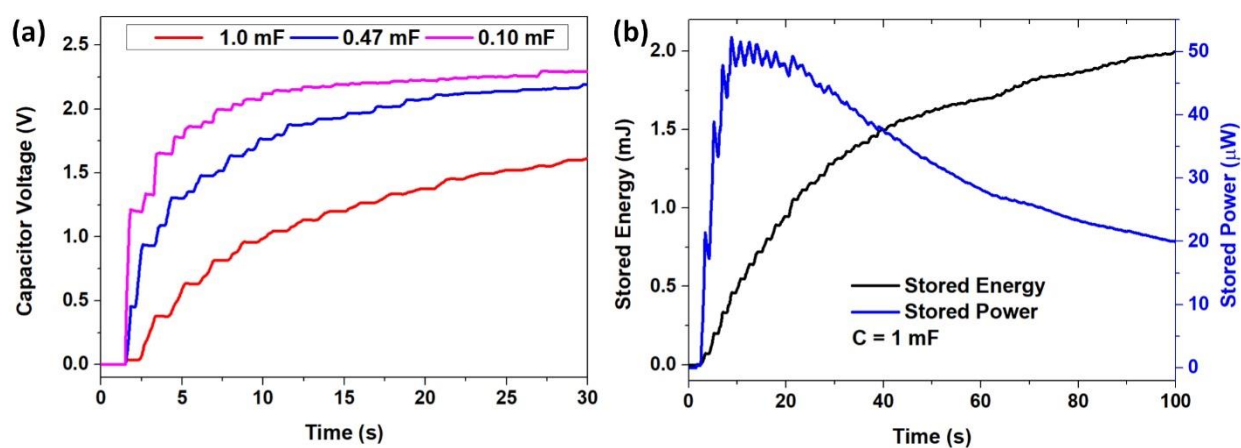


Figure S9. (a) Charging behaviors of six-unit cells of SLITF-TEG at different load capacitances. (b) Stored energy-time and stored power-time relationships for a fixed capacitor of 1 mF.

Video S1: Measurement of the open-circuit voltage

Video S2: Measurement of the short-circuit current

Video S3: SLITF-TEG directly charges a 6.8 mF capacitor

Video S4: Six-unit cells of SLITF-TEG directly power a light-emitting diode